Reports

Ozone Monitoring with an Infrared Heterodyne Radiometer

Abstract. *Measurements of the total burden and of the concentration versus altitude profiles of ozone have been made with a ground-based heterodyne radiometer at Pasadena, California. The measurements were made in the 9.5-micrometer wavelength region, where a strong ozone infrared absorption band exists. The radiometer measured solar absorption at selected wavelengths, with a spectral resolution of 0.001 reciprocal centimeter, equivalent to the half-width of an ozone absorption line at the 10-millibar altitude level. A carbon dioxide laser served as the local oscillator. This technique can be used to gather important data on both tropospheric and stratospheric ozone, which are not readily accessible with other remote-sensing techniques.*

Recent conclusions that the stratospheric O_3 layer might be perturbed by man-made pollutants, such as oxides of nitrogen (NO_x) and chlorofluoromethanes (*1*), point toward the need for an improved O_3 monitoring network. Since there are both temporal and spatial variations in the O_3 distribution, a combination of techniques must be exploited in the future in order to assess man's influence on O_3 and the consequent biological (*2*) and climatic (*3*) effects of an O_3 density perturbation.

An instrument such as a solar heterodyne radiometer (*4, 5*), operating at wavelengths in the ν_3 band of O_3 near 9.5 μm, has a unique ability to accurately measure both the total burden and the concentration versus altitude profile of O_3 from a remote location. The basic sensitivity of this type of radiometer to O_3 is high, because unattenuated solar radiation produces a high signal-to-noise (S/N) ratio, and the stronger individual O_3 lines in this infrared band produce an absorption of a few percent for a column abundance as small as 10 parts per billion–kilometers, at altitudes from 0 to 35 km. Unlike the Dobson instrument, the infrared heterodyne radiometer is unaffected by tropospheric aerosols. The O_3 lines in this spectral region are pressure-broadened up to an altitude of about 35 km; by using the heterodyne radiometer to scan through an O_3 absorption line with enough spectral resolution to resolve the line at this altitude, one can determine the relative contributions of O_3 molecules at various altitudes to the total absorption line shape (*6*). Above 35 km, Doppler-broadening becomes predominant and both the sensitivity and the ability to profile the O_3 fall off with increasing altitude. The O_3 number density also falls off rapidly with increasing altitude in this region, and the profile is relatively well behaved and determined by photochemical reactions; thus the contribution to the total burden from this region is small and more predictable than the contribution from O_3 at lower altitudes. Another proposed O_3 monitoring technique, based on the use of millimeter wave receivers (*7*), is complementary to the infrared technique because its profiling accuracy is good in the altitude region from 25 to 80 km. Below 25 km, the overlap or blending of the various atmospheric absorption lines becomes a severe problem in this spectral region. Base-line errors are also more significant when measurements with a millimeter wave receiver are made over a frequency range corresponding to a lower altitude linewidth.

A $^{12}C^{16}O_2$ laser was used as a local oscillator. This laser was grating-tunable from line to line, so that several spectral regions in the O_3 ν_3 band could be used for measurements. The photomixer and intermediate frequency (IF) electronics were chosen so that a total bandwidth of 600 Mhz (0.02 cm^{-1}) was available, with a 30-Mhz (0.001 cm^{-1}) resolution within this bandwidth. This spectral resolution is equivalent to the half-width of a Doppler-broadened O_3 line at typical stratospheric temperatures in the 35-km altitude region. The local oscillator and photomixer were the same as those described in earlier measurements of thermal radiation from various pollutant gases (*8*). The amplitude stability of the local oscillator was sufficient for receiver operation near the quantum noise limiting sensitivity. Under these conditions, the S/N ratio which can be obtained when looking at the sun through an absorbing gas is (*5*):

$$S/N = (\sqrt{2}/\pi)\,\eta\,(\tau B_{IF})^{1/2} \times [\exp(hf/kT) - 1]^{-1} \exp[-u(f)\sec\psi] \quad (1)$$

where η is the quantum efficiency including optical reflection losses, τ is the post-detection integration time, B_{IF} is the IF bandwidth, h is Planck's constant, f is the frequency of the radiation emitted by a source at temperature T, k is Boltzmann's constant, $u(f)$ is the zenith optical thickness of the atmosphere, and ψ is the angle of the sun with respect to the zenith. The optical thickness is given by

$$u(f) = \int N(z)\,\sigma(f,z)\,dz \quad (2)$$

where the integral is over the entire atmospheric thickness, $N(z)$ is the number density of the absorbing gas, and $\sigma(f,z)$ is the absorption cross section of the absorbing gas. When the atmosphere is transparent at a frequency f corresponding to a wavelength near 10 μm, the S/N ratio for $B_{IF} = 30$ Mhz and $\tau = 10$ seconds is 10^4 (40 db). There is very little change in the S/N ratio in the "atmospheric window" region from 8 to 14 μm, the increase being about a factor of 2 as the viewing wavelength is increased from 8 to 14 μm.

When the O_3 measurements were taken, on several days during the winter of 1976, the local oscillator of the heterodyne receiver was operated on the P(18) through P(24) lines of the 9.4-μm band of the CO_2 laser. Moderately strong O_3 lines exist with ± 0.02 cm^{-1} of the P(18) and P(24) line frequencies at 1048.661 and 1043.163 cm^{-1}, respectively. The corresponding regions around the P(20) and P(22) lines do not contain any O_3 lines of significance; thus the O_3 absorption in these regions is predominantly due to wings of strong O_3 lines that are within 0.2 cm^{-1} of the laser line frequencies. Thus the observing wavelengths in the P(20) and P(22) regions (1046.8543 and 1045.002 cm^{-1}, respectively) can be used to selectively measure O_3 in the altitude region from 0 to 12 km, where the O_3 linewidths are large enough to influence the solar absorption. Figure 1 is a portion of the O_3 absorption spectrum near the P(24) CO_2 laser line, indicating the presence of an O_3 line at 1043.183 cm^{-1}, or 0.02 cm^{-1} above the P(24) local oscillator frequency. It is obvious that the O_3 at higher altitudes contributes to absorption only in small spectral intervals, such that independent measurements in wing regions (for example, 1043.163 cm^{-1}) and in line center regions (for example, 1043.183 cm^{-1}) can be used to discrimi-

Scoreboard for Reports. We have an uncomfortably large backlog of accepted Reports that await publication. For the past several months we have accepted about 17 Reports per week, a little more than 25 percent of those submitted. In order to reduce the backlog and shorten the publication delay, we will accept only 12 papers per week for the next few months.

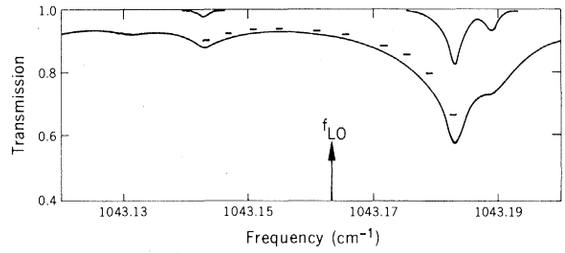

Fig. 1. Zenith solar absorption due to O_3, in the frequency region near the $^{12}C^{16}O_2$ laser line at 1043.163 cm^{-1}. The solid lines are calculations, based on the use of the mid-latitude summer model for O_3 with a number density peak at 22 km (*13*). The upper trace indicates transmission through the altitude portion from 30 to 33 km only, whereas the lower trace indicates transmission through the entire O_3 layer. The dashes are measurements made on 15 January 1976, corrected to remove the effects of the solar slant path and the CO_2 absorption. These measurements were made with a tunable receiver with a bandwidth of 30 Mhz (0.001 cm^{-1}). The measurements indicated here were made at the frequencies $f_{LO} \pm 60$, 270, 360, 480, and 600 Mhz, with 10-second integration times at each frequency.

nate between low- and high-altitude O_3. The altitude resolution that can be obtained with this technique depends on the number of sensing channels, until the number of channels becomes larger than seven or eight; in this case the resolution, typically 4 to 5 km in the stratosphere, is limited by the widths of the weighting functions, $\sigma(f,z)$ (see Eq. 2), when these functions are plotted as functions of z at a fixed frequency f (*6*).

Figure 2 shows an O_3 profile generated from measurements taken at Pasadena, California, on 15 January 1976. In order to generate this profile from the solar absorption measurements, and iterative technique (*6, 9*) was used. In brief, what is desired is the inverse solution to Eq. 2 or a related integral equation in which pressure replaces altitude as the independent variable. According to the iterative technique that was used, a set of pressure levels is selected so that each sensing frequency is used to calculate the O_3 concentration at a particular pressure level. An initial guess as to the altitude profile is then made. A set of absorption coefficients is generated based on the initial guess, and a comparison is made with the measured absorption coefficients. A new profile is generated based on the relation

$$|q'(p_i)| \,/\, |q^\circ(p_i)| = |u_a(f_i)| \,/\, |u_c(f_i)| \quad (3)$$

where $q'(p_i)$ is the new value for the O_3 mixing ratio at pressure level i, $q^\circ(p_i)$ is the old value of that ratio, and $u_a(f_i)$ and $u_c(f_i)$ are the actual and computed values for optical thickness at frequency f_i. Several iterations are carried out until the residual differences between u_a and u_c fall below a preselected value. In the analysis of the measurements made on 15 January, initial guesses which peaked at various altitudes were used. The profile pictured in Fig. 2 produced the smallest residual after a fixed number of iterations. The retrieved profiles produced values for the total O_3 burden which were within 10 percent of each other, regardless of the initial guess. The total O_3 burden for this 15 January data was 0.23 atm-cm. (The measurements from which Fig. 2 was generated were taken near 2:00 p.m.) The 5- to 6-km altitude resolution of the O_3 profile is not surprising in view of the fact that only four independent sensing channels were used to generate the profile on the particular day. In view of the limitations in altitude resolution discussed earlier, the ultimate ambiguity, even if several more channels were used, would remain around 4 km.

It became apparent during the analysis of the data that the heterodyne radiometer measurement technique for generating O_3 profiles is very sensitive to inaccuracies in the spectral line parameters which are used in the calculations. Initial attempts at generating profiles based on measurements taken in the month of Janaury produced results which deviated considerably from expected profiles for this location and time of year. We undertook a program during the spring to improve the accuracies of the listed O_3 line frequencies in the spectral regions of interest, using a CO_2 wave-guide laser with a large tuning width (*10*). As a result, O_3 line frequencies were found to be from 0.003 to 0.006 cm^{-1} lower than those listed in the Air Force Cambridge Research Laboratories compilation (*11*), which is a small error for conventional infrared instruments but very large for this work [see (*10*) for details]. Using the new values for the O_3 line parameters greatly improved the O_3 profiling results. Further laser spectroscopy of O_3 would be valuable in refining the accuracy of this technique and in expanding the flexibility of this instrument to operate at a number of other sensing frequency regions.

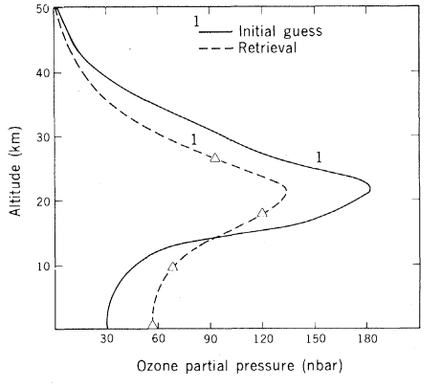

Fig. 2. The O_3 profile measured at 1400 P.S.T. on 15 January 1976. The initial guess used in the retrieval calculation (see text) is also shown. The total O_3 burden measured was 0.23 atm-cm. The ambient air temperature was 76°F (297°K) when the measurement was made. The triangles indicate altitudes at which the retrieval calculations were made. A shape-preserving interpolation was used to connect these points.

Comparison of these solar heterodyne radiometer measurements with other measurements of the total burdens and the altitude profiles of O_3 have been difficult to make because of the scarcity of data taken in the western United States. The nearest continuously operating Dobson instruments (which measure the total O_3 burden) are at White Sands, New Mexico, and Boulder, Colorado. [The peak O_3 readings on 15 January were reported to be 0.307 atm-cm at Boulder and 0.323 atm-cm at White Sands (*12*), compared with our reading of 0.23 atm-cm at 1400 P.S.T.] The construction of a transportable solar heterodyne radiometer is under way. Joint measurements with ozonesondes and Dobson instruments should be carried out in order to assess and further develop the capabilities for monitoring O_3.

ROBERT T. MENZIES
Jet Propulsion Laboratory,
California Institute of Technology,
Pasadena, California 91103
ROBERT K. SEALS, JR.*
NASA Langley Research Center,
Hampton, Virginia 23665

References and Notes

1. H. Johnston, *Science* **173**, 517 (19 → M. B. McElroy, S. C. Wofsy, J. E. Pennar, J. C. McConnell, *J. Atmos. Sci.* **31**, 287 (1974); M. J. Molina and F. S. Rowland, *Nature (London)* **249**, 810 (1974); R. J. Cicerone, R. S. Stolarski, S. Walters, *Science* **185**, 1165 (1974); P. J. Crutzen, *Geophys. Res. Lett.* **1**, 205 (1974).
2. P. Cutchis, *Science* **184**, 13 (1974); F. Urbach and R. E. Davies, in *Proceedings of the Fourth Conference on the Climatic Impact Assessment Program*, T. M. Hard and A. J. Broderick, Eds. (U.S. Department of Transportation, Washington, D.C., 1975), p. 66.
3. V. Ramanathan, L. B. Callis, R. E. Boughner, *J. Atmos. Sci.* **33**, 1092 (1976).
4. B. J. Peyton, A. J. DiNardo, S. C. Cohen, J. H. McElroy, R. J. Coates, *IEEE J. Quantum Electron.* **QE-11**, 569 (1975).
5. R. T. Menzies, in *Laser Monitoring of the Atmosphere*, E. D. Hinkley, Ed. (Springer, Berlin, 1976), p. 297.
6. _____ and M. T. Chahine, *Appl. Opt.* **13**, 2840 (1974).
7. F. I. Shimabukuro, personal communication.
8. R. T. Menzies and M. S. Shumate, *Science* **184**, 570 (1974).

9. M. T. Chahine, *J. Atmos. Sci.* **27**, 960 (1970).
10. R. T. Menzies, *Appl. Opt.* **15**, 2597 (1976).
11. R. A. McClatchey, W. S. Benedict, S. A. Clough, D. E. Burch, R. F. Calfee, K. Fox, L. S. Rothman, J. S. Garing, *Atmospheric Absorption Line Parameters Compilation* (publication AFCRL-TR-73-0096, Air Force Cambridge Research Laboratories, Bedford, Mass., January 1973).
12. R. D. Grass, personal communication.
13. R. A. McClatchey, R. W. Fenn, J. E. A. Selby, F. E. Volz, J. S. Garing, *Optical Properties of the Atmosphere (Revised)* (publication AFCRL-TR-71-0279, Air Force Cambridge Research Laboratories, Bedford, Mass., 1971).
14. We thank M. Shumate for helpful suggestions. A portion of this work was supported under NASA contract NAS-7-100.
* Present address: National Aeronautics and Space Administration, Washington, D.C. 20546.

9 December 1976; revised 23 May 1977

The Prime Meridian of Mars and the Longitudes of the Viking Landers

Abstract. *A new planetwide control net of Mars has been computed by a single large-block analytical triangulation derived from 17,224 measurements of 3,037 control points on 928 Mariner 9 pictures. The computation incorporated the new Viking-determined direction of the spin axis and rotation rate of Mars. The angle* V, *measured from the vernal equinox to the prime meridian (areocentric right ascension) of Mars, was determined to be* $V = 148.368° + 350.891986° (JD - 2433282.5)$, *where JD refers to the Julian date. The prime meridian of Mars passes through the center of the small crater Airy-O. The longitudes of the Viking landers are* $\lambda_1 = 47.82° \pm 0.1°$ *and* $\lambda_2 = 225.59° \pm 0.1°$.

A new coordinate system for Mars was defined after the Mariner 9 mission (*1*). This coordinate system included a new direction for the spin axis, a new rotation rate, a new reference spheroid for cartographic purposes, and a new prime meridian defined as the meridian passing through the center of a small crater called Airy-O. The system was adopted by the International Astronomical Union at its General Assembly in Sydney in 1973 (*2*) and is used on all modern maps of Mars (*3*).

Analysis of the radio tracking data from the Viking 1 and Viking 2 landers has resulted in improved values for the direction of the spin axis and the rotation rate of Mars (*4*). The location of the lander sites was also determined very accurately relative to the vernal equinox of Mars and in terms of latitude and areocentric radii. The best method of determining the longitudes of the landers is by means of a photogrammetric tie to Airy-O. However, because it has not been possible to identify the lander locations on orbiter pictures, this approach has not been feasible. This inability to find the lander locations relative to the local topography is a shortcoming of the Viking mission, and care should be taken in the future to be sure that landers and rovers can be located with reference to the local terrain. A less direct method of determining the longitudes of the landers is to measure the angle between the prime meridian and vernal equinox by treating this angle as an unknown in the least-squares computation of the planetwide control net (*5*). This method has always been used in the past as there was no hope of obtaining independently determined accurate coordinates of such points as landers.

A new planetwide control net of Mars has been computed by a single large-block analytical triangulation derived from 17,224 measurements of 3,037 control points on 928 Mariner 9 pictures. The computation incorporated the new Viking-determined direction of the spin axis and rotation rate of Mars (*4*). The photogrammetric method has been described elsewhere (*5*). The least-squares computation resulted in improved values of latitude and longitude of the control points and orientation angles of the pictures. The spacecraft coordinates when the pictures were taken were obtained from the Jet Propulsion Laboratory Science Data Team and were assumed correct in the computation. The areocentric radii at the control points were derived from three sources: 2,163 were interpolated from occultation measurements and used in past control net computations (*5*), 22 were computed photogrammetrically (*6*), and 852 were derived from elevations on the available U.S. Geological Survey 1:5,000,000 topographic series of Mars maps (MC-4, MC-10, MC-11, MC-17, MC-18, MC-19, and MC-23). The elevation contours on these maps were derived from analysis of many sources of data (*7*). The analytical triangulation required the solution of 8,858 normal equations. The standard error of the measurements was 0.0167 mm or slightly more than one pixel (0.0144 mm).

This control net computation determined the angle from the Mars vernal equinox to the prime meridian to be

$$V = 148.368° + 350.891986° (JD - 2433282.5)$$

where JD is the Julian date and 2433282.5 is the Julian date of the reference epoch 1950 January 1.0 Ephemeris Time. On the basis of the value of V, the longitudes of the Viking landers are (*4*) $\lambda_1 = 47.82° \pm 0.1°$ and $\lambda_2 = 225.59° \pm 0.1°$.

MERTON E. DAVIES
Rand Corporation,
Santa Monica, California 90406

References and Notes

1. G. de Vaucouleurs, M. E. Davies, F. M. Sturms, Jr., *J. Geophys. Res.* **78**, 4395 (1973).
2. "Physical study of planets and satellites," in *Proceedings, 15th General Assembly, 1973: International Astronomical Union Transactions* (International Astronomical Union, Thessaloniki, Greece, 1974), vol. 14B, p. 107.
3. R. M. Batson, *J. Geophys. Res.* **78**, 4424 (1973).
4. W. H. Michael, Jr., *et al.*, *Science* **194**, 1337 (1976); A. P. Mayo, W. T. Blackshear, R. H. Tolson, W. H. Michael, Jr., G. M. Kelly, J. P. Brenkle, T. Komarek, *J. Geophys. Res.*, in press.
5. M. E. Davies and D. W. G. Arthur, *J. Geophys. Res.* **78**, 4355 (1973); M. E. Davies, *Photogramm. Eng.* **39**, 1297 (1973); *Mariner 9 Control Net of Mars: May 1974* (Report R-1525-NASA, Rand Corporation, Santa Monica, Calif., May 1974).
6. M. E. Davies, *Icarus* **21**, 230 (1974).
7. S. S. C. Wu, *Topographic Mapping of Mars* (Interagency Report: Astrogeology 63, U.S. Geological Survey, Washington, D.C., 1975).
8. This research was supported by contract NASW-3017, Planetary Geology Office, National Aeronautics and Space Administration.

16 May 1977; revised 23 June 1977

Cholera Toxin Crystals Suitable for X-ray Diffraction

Abstract. *Large crystals of the cholera toxin were grown; their dimensions, symmetry* ($P2_1$), *order, and resistance to radiation make them ideally suited for a high-resolution x-ray structure determination. There is one molecule (approximately 84,000 daltons) per asymmetric unit, and therefore the lattice reveals no molecular symmetry. Two distinct bioassays indicate that the protein from dissolved crystals retains full biological activity.*

We report here the preparation of cholera toxin (CT) crystals which are quite suitable for a high-resolution x-ray crystallographic structure determination. Cholera toxin is a protein exotoxin which, when released by the *Vibrio cholerae* in the small bowel, produces a noninflammatory secretory diarrhea (*1*). The massive secretion of salt and water is triggered by the binding of the toxin to